Developmental Cell
Article

# ADF/Cofilin Regulates Secretory Cargo Sorting at the TGN via the $Ca^{2+}$ ATPase SPCA1

Julia von Blume,[1] Anne-Marie Alleaume,[1] Gerard Cantero-Recasens,[2] Amy Curwin,[1] Amado Carreras-Sureda,[2] Timo Zimmermann,[1] Josse van Galen,[1] Yuichi Wakana,[1] Miguel Angel Valverde,[2] and Vivek Malhotra[1,3,*]
[1]Department of Cell and Developmental Biology, Centre de Regulacio Genomica, 08003 Barcelona, Spain
[2]Laboratory of Molecular Physiology and Channelopathies, Department of Experimental and Health Sciences, Universitat Pompeu Fabra, 08003 Barcelona, Spain
[3]Institucio Catalana de Recerca I Estudis Avancats, 08010 Barcelona, Spain
*Correspondence: vivek.malhotra@crg.es
DOI 10.1016/j.devcel.2011.03.014

## SUMMARY

**Actin-severing proteins ADF/cofilin are required for the sorting of secretory cargo at the trans-Golgi network (TGN) in mammalian cells. How do these cytoplasmic proteins interact with the cargoes in the lumen of the TGN? Put simply, how are these two sets of proteins connected across the TGN membrane? Mass spectrometry of cofilin1 immunoprecipitated from HeLa cells revealed the presence of actin and the $Ca^{2+}$ ATPase SPCA1. Moreover, cofilin1 was localized to the TGN and bound to SPCA1 via dynamic actin. SPCA1 knockdown, like ADF/cofilin1 knockdown, inhibited $Ca^{2+}$ uptake into the TGN and caused missorting of secretory cargo. These defects were rescued by the overexpression of the TGN-localized SPCA1. We propose that ADF/cofilin-dependent severing of actin filaments exposes and promotes the activation of SPCA1, which pumps $Ca^{2+}$ into the lumen of the TGN for the sorting of the class of secretory cargo that binds $Ca^{2+}$.**

## INTRODUCTION

The Golgi apparatus is essential for the sorting and transport of newly synthesized proteins arriving from the endoplasmic reticulum (ER) (Pfeffer, 2007). All newly synthesized pools of proteins enter the Golgi stack at the *cis* face, and those containing a KDEL sequence are retrieved by KDEL receptor to the ER in COPI-coated vesicles (Lewis and Pelham, 1990). In the most distal Golgi compartment, conveniently called the trans-Golgi network (TGN), the Mannose-6-phosphate–containing lysosomal hydrolases bind Mannose-6-phosphate receptor (M6PR) and are transported to the endosomes/lysosomes in clathrin-coated vesicles (Baranski et al., 1990). How are the soluble secretory proteins, which are destined for secretion in the extra cellular space, sorted and exported from the Golgi apparatus? More specifically, is the sorting and packing of secretory cargoes receptor mediated?

A genomewide screen for defects in secretion of the soluble secretory protein signal sequence (ss)–HRP revealed the requirement of the actin-severing protein twinstar in *Drosophila* S2 cells (Bard et al., 2006). Knockdown of twinstar by RNAi arrested HRP in the TGN. Similarly, knockdown of the twinstar orthologs ADF and cofilin1, which are expressed in HeLa cells, arrested ss-HRP in the TGN (von Blume et al., 2009). This was not due to a defect in the budding of HRP-containing transport carriers, because secretion of a number of other secretory proteins was unaffected under such conditions. Because the lysosomal hydrolase Cathepsin D and the Golgi resident $Ca^{2+}$-binding protein Cab45 were secreted upon knockdown of ADF and cofilin1, we proposed that these proteins are required for sorting of secretory cargo at the TGN (von Blume et al., 2009). How can ADF and cofilin1, which are cytoplasmic proteins, regulate the sorting of the lumenal secretory content of the TGN? We hypothesized that an actin patch on the cytoplasmic surface of the TGN segregates molecular sorters (integral membrane proteins), which in turn regulate the physiology of the lumenal milieu of the TGN. Disorganization of the actin patch upon knockdown of ADF and cofilin1 affected the activity of the molecular sorters and therefore the sorting of the lumenal contents of the TGN. The molecular sorters, we proposed, might be different forms of ion transporters (e.g., ions pumps or channels) that could potentially regulate pH and $Ca^{2+}$ gradients across the TGN (von Blume et al., 2009).

We now provide evidence that ADF/cofilin-dependent cargo sorting at the TGN requires the activity of the secretory pathway calcium ATPase 1 (SPCA1). We describe our findings on the interaction between these two proteins via dynamic actin to control $Ca^{2+}$ homeostasis, which is necessary for the secretory cargo sorting at the TGN.

## RESULTS

### ADF/Cofilin Interacts with Actin and SPCA1 and Regulates the Sorting of Secretory Cargo at the TGN

To gain a better understanding of the role of ADF/cofilin in secretory cargo sorting at the TGN, we sought to identify the interacting partners of cofilin1. Cofilin1 was immunoprecipitated from HeLa cell lysates, and the immunoprecipitated proteins were analyzed by mass spectrometry (MS). Besides actin, which is known to bind cofilin, several peptides of SPCA1 were identified in the MS analysis (Figure 1A). SPCA1 localizes to the TGN and is known to be required for $Ca^{2+}$ import into the TGN (Gunteski-Hamblin et al., 1992; Lissandron et al., 2010; Sepulveda et al., 2009; Vanoevelen et al., 2005a, 2005b). In addition, because

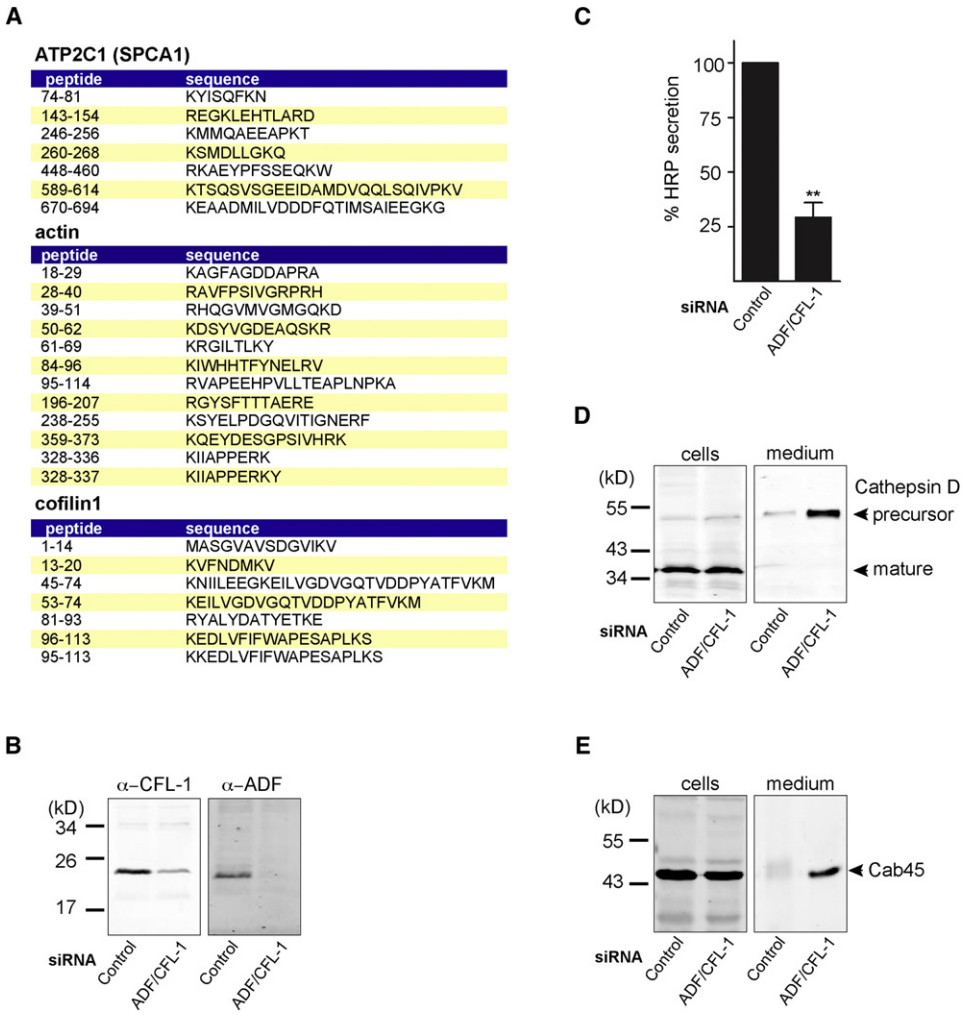


**Figure 1. ADF/Cofilin Interacts with Actin and SPCA1 and Regulates the Sorting of Secretory Cargo at the TGN**

(A) HeLa cells were lysed and clarified by centrifugation. The supernatant was immunoprecipitated with an anti-cofilin1 antibody and the immunoprecipitate was analyzed by mass spectrometry. In addition to the peptides of cofilin1, actin- and SPCA1-specific peptides were contained in the immunoprecipitate.

(B–E) Lysates of HeLa cells stably expressing ss-HRP transfected with control or ADF/cofilin1 siRNA were analyzed by western blotting using anti-cofilin1, ADF (B), Cathepsin D (D), and Cab45 (E) antibodies. The media from control and ADF/cofilin1 siRNA transfected cells were also used to monitor the levels of HRP activity (C). Compared datasets were termed as statistically significant with p values of $< 0.01$ (**). Error bars indicate the mean SD of HRP activity in the medium normalized with respect to the HRP activity in the cell lysates.

many of the missorted secretory cargoes upon ADF/cofilin1 knockdown by siRNA were $Ca^{2+}$-binding proteins (e.g., Cab45, Follistatin-related protein 4, Nidogen-1, Proprotein convertase subtilisin/kexin type 9, and Thrombospondins 1 and 3) and because $Ca^{2+}$ homeostasis at the Golgi is known to play a role in processing and secretion of secretory cargo, we hypothesized that SPCA1-dependent $Ca^{2+}$ import into the TGN was important for the ADF/cofilin-actin–dependent sorting of secretory proteins.

We first reassessed the effect of the knockdown of ADF/cofilin1 on secretory cargo sorting. HeLa cells stably expressing ss-HRP were transfected with control or specific siRNAs to knockdown both ADF and cofilin1, as described previously (von Blume et al., 2009). The cell lysates were western blotted with the respective antibodies to monitor the knockdown efficiency. The knockdowns of cofilin1 and ADF were estimated at 80% and 90%, respectively, compared with control cells (Figure 1B). HRP activity in the medium from the cells was measured by a chemiluminescence procedure described previously (von Blume et al., 2009). Knockdown of ADF/cofilin1 inhibited secretion of HRP (Figure 1C). Western blotting of the medium and the cell lysates revealed that Cathepsin D and Cab45 were secreted upon ADF/cofilin1 knockdown (Figures 1D and 1E). These findings confirm our previous data on the requirement of ADF/cofilin1 for the sorting of secretory cargo at the TGN (von Blume et al., 2009). Location of these three proteins was therefore used as an assay to detect sorting defects.

## SPCA1-Dependent $Ca^{2+}$ Homeostasis Is Required for Cargo Sorting at the TGN

HeLa cells were stained with an anti-SPCA1 antibody and visualized by confocal microscopy. SPCA1 showed a clear colocalization with the TGN marker TGN46 (Figure 2A). The involvement

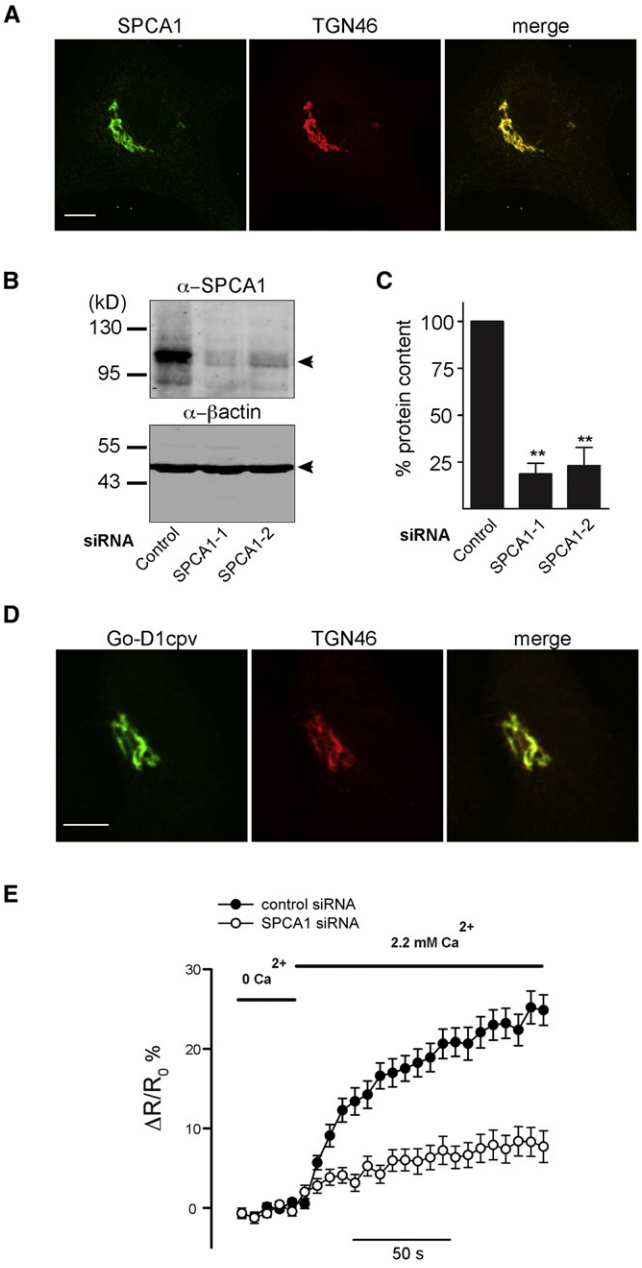


**Figure 2. $Ca^{2+}$ Homeostasis of the TGN Is Controlled by SPCA1**

(A) HeLa cells were visualized by fluorescence microscopy with SPCA1- and TGN46-specific antibodies (size bars represent 5 μm).

(B) Lysates of HeLa cells transfected with control or SPCA1-specific siRNA were western blotted with anti-SPCA1 (top panel) and actin antibodies (bottom panel).

(C) The effect of SPCA1 siRNAs (SPCA-1 and SPCA1-2) was quantified using the ImageJ software and was normalized to the expression of SPCA1 compared with cells transfected with control siRNA. Bar graphs represent the mean ± SD of triplicate experiments. Compared datasets were statistically significant (**) when $p < 0.01$.

(D) HeLa cells were transfected with the TGN-specific $Ca^{2+}$ FRET sensor Go-D1cpv, fixed, and stained with an anti-TGN46 antibody. (E) Cells treated with control and SPCA1 siRNAs were cotransfected with Go-D1cpv. $Ca^{2+}$ entry into the TGN was measured in $Ca^{2+}$-depleted cells transfected with control siRNA (n = 38) or SPCA1 siRNA (n = 16). Fluorescent signals reflecting TGN [$Ca^{2+}$] were presented as $\Delta R/R_0$, where $R_0$ is the value obtained before addition of 2.2 mM $Ca^{2+}$ to the cells bathing solution. Data are expressed as the mean ± SEM. Mean maximum values measured after readdition of $Ca^{2+}$ were statistically different between control and SPCA1 siRNA (24 ± 2% and 8 ± 2%, respectively; $p < 0.01$) (n = number of cells monitored).

See also Figure S1.

of SPCA1 in $Ca^{2+}$ import into the TGN was evaluated in HeLa cells transfected with siRNA oligos to knock down SPCA1. This procedure resulted in the knockdown of SPCA1 by 80% compared with control cells (Figures 2B and 2C).

A direct measurement of the $Ca^{2+}$ concentration within the lumen of the TGN was evaluated using a fluorescence resonance energy transfer (FRET)–based $Ca^{2+}$ sensor (Go-D1cpv) that is targeted to the TGN, thus permitting the direct involvement of SPCA1 in the calcium homeostasis of the TGN (Lissandron et al., 2010). To perform $Ca^{2+}$ measurements, HeLa cells were transfected with scrambled- or SPCA1-specific siRNAs followed by Go-D1cpv transfection after 48 hr. This genetically encoded $Ca^{2+}$ indicator is targeted to the trans-Golgi (Figure 2D). Measurement of the $Ca^{2+}$ concentration in the Golgi was carried out by detecting the FRET efficiency between CFP and YFP linked by a modified Calmodulin and Calmodulin-binding domain, as recently described (Lissandron et al., 2010). Fluorescent signals reflecting TGN [$Ca^{2+}$] were presented as $\Delta R/R_0$ ($\Delta R$ = change in the ratio of YFP/CFP emission intensity at any time, and $R_0$ is the value obtained before addition of 2.2 mM $Ca^{2+}$ to the bathing solution of cells that had been previously depleted of $Ca^{2+}$). The results revealed that compared with control cells, $Ca^{2+}$ uptake in the TGN of SPCA1 knockdown cells was greatly reduced (Figure 2E). This experiment was carried out with both SPCA1 specific siRNAs, and the results were similar (data not shown). The effect of SPCA1 knockdown on the intracellular $Ca^{2+}$ signals generated at the Golgi was also evaluated using an indirect method based on the measurement of the cytosolic [$Ca^{2+}$] with Fura-2 (Lissandron et al., 2010) (see Figures S1A and S1B, available online).

Next, the role of SPCA1 in protein sorting at the TGN was tested. HeLa cells stably expressing ss-HRP were depleted of SPCA1, and the cell culture medium was collected to detect Cathepsin D and Cab45 by western blotting with the respective antibodies (Figures 3A and 3B). The medium from these cells was also tested for HRP activity by chemiluminescence (Figure 3C). SPCA1 knockdown caused secretion of Cathepsin D and Cab45 and inhibited the secretion of HRP from HeLa cells. Furthermore, the localization of HRP, in control and SPCA1 siRNA–treated cells, after arresting the cargo in the TGN (by incubation at 20°C) and staining with an HRP antibody was analyzed. At 20°C, HRP was contained in the TGN of both the control and SPCA1 knockdown cells. Cells were then shifted to the permissive temperature of 32°C, stained, and visualized with anti-HRP antibody by confocal microscopy. Upon this temperature shift, HRP was exported from the Golgi in control cells but remained in the TGN of SPCA1 knockdown cells (Figure 3D). The effect of SPCA1 knockdown on HRP localization was visualized by confocal microscopy and quantified by counting 100 cells in at least three different experiments (Figure 3E).

The specific effect of SPCA1 knockdown on $Ca^{2+}$ import into the TGN and the secretory cargo sorting was further tested by rescue experiments with an SPCA1 siRNA–resistant mutant

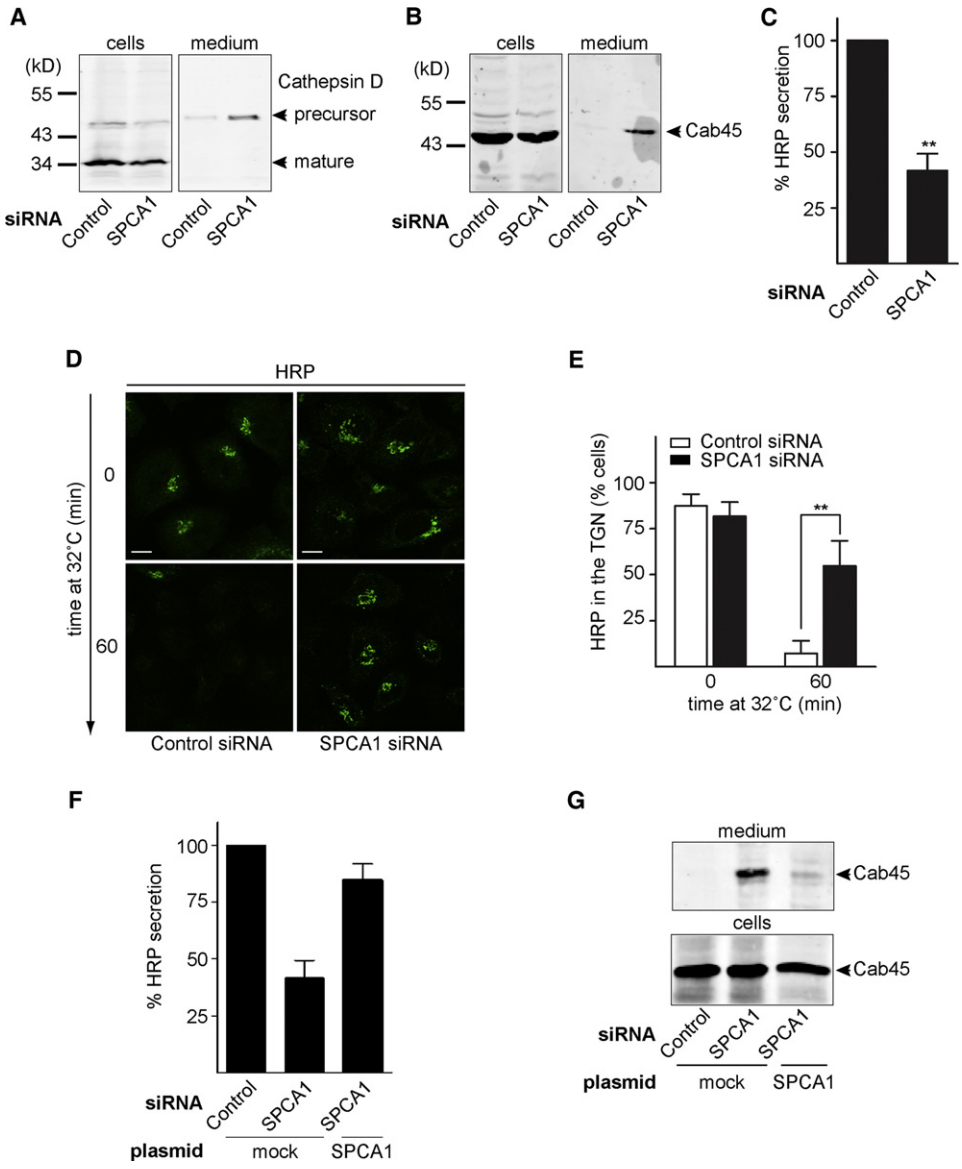


**Figure 3. SPCA1 Knockdown Causes Missorting of Secretory Cargo**

(A and B) Cell lysates and medium of control and SPCA1 knockdown HeLa cells stably expressing ss-HRP were western blotted with anti–Cathepsin D (A) and Cab45 (B) antibodies.

(C) The media from control and SPCA1 knockdown cells were also used to detect HRP by chemiluminescence. Error bars indicate mean ± SD of HRP activity in the medium normalized by HRP activity in cell lysates of triplicate measurements from representative experiments. Compared datasets were termed as statistically significant when $p < 0.01$ (**).

(D) HeLa cells stably expressing ss-HRP were transfected with control and SPCA1-specific siRNA and were incubated at 20°C for 2 hr. The cells were then shifted to 32°C, and the localization of HRP was monitored by fluorescence microscopy with an anti-HRP antibody (size bars represent 5 μm).

(E) One hundred cells were counted to quantitate the location of HRP in control and SPCA1 knockdown ss-HRP expressing HeLa cells. Bar graphs represent data from at least three different experiments.

(F and G) Cells were transfected with control and SPCA1 siRNA. After 24 hr, cells were transfected either with a mock plasmid or SPCA1 wild-type. Secretion of HRP (F) and Cab45 (G) was monitored as described above.

See also Figure S2.

(Figure S2A). Expression of siRNA-resistant wild-type SPCA1 rescued almost completely the defects in $Ca^{2+}$ uptake into the TGN (Figures S2B and S2C) and the sorting of HRP and Cab45 (Figures 3F and 3G). Together, these findings support the role of SPCA1-dependent $Ca^{2+}$ uptake into the TGN in the sorting of secretory cargo.

## ADF/Cofilin1 Knockdown Affects $Ca^{2+}$ Import into the TGN

Because SPCA1 knockdown affected cargo sorting at the TGN, we tested whether ADF and cofilin1 have a role in $Ca^{2+}$ import into the TGN and if it was coupled to the activity of SPCA1. HeLa cells were transfected with control or ADF/cofilin1 siRNAs, as

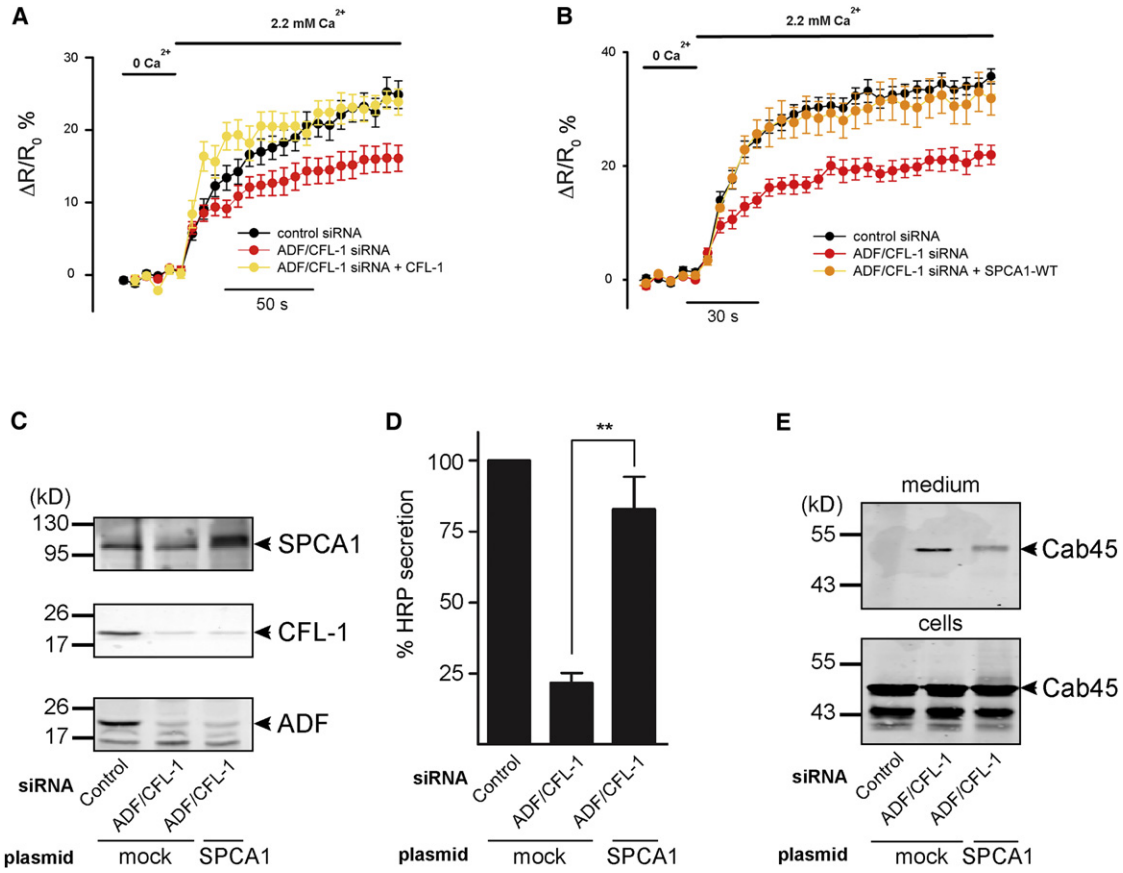


**Figure 4. Knockdown of ADF and Cofilin1 Affects $Ca^{2+}$ Homeostasis of the TGN**

(A) HeLa cells transfected with control (n = 38) or ADF/cofilin1-specific siRNA and a mock plasmid (n = 26) or an siRNA-resistant mutant of cofilin1 (n = 9) were cotransfected with the TGN-specific $Ca^{2+}$ sensor Go-D1cpv. TGN measurements were performed as described in Figure 2E. Mean maximum values after readdition of $Ca^{2+}$ were statistically different between control and ADF/cofilin1 siRNA (24 ± 2% and 16 ± 2%, respectively; $p < 0.01$) but not between control and ADF/cofilin siRNA+cofilin1 (23 ± 1; $p > 0.05$).

(B) Cells were transfected with control (n = 12) or ADF/cofilin1 siRNAs and a mock plasmid (n = 7) or SPCA1 wild-type (n = 8) and Go-D1cpv. $Ca^{2+}$ entry into the TGN was measured using the Go-D1cpv probe. Mean maximum values after readdition of $Ca^{2+}$ were statistically different between control and ADF/cofilin1 siRNA (35 ± 1% and 21 ± 1%, respectively; $p < 0.01$) but not between control and ADF/cofilin1 siRNA+SPCA1-WT (31 ± 1%; $p > 0.05$) (n = number of cells monitored).

(C) Cells treated with control or ADF/cofilin1 siRNAs and a mock plasmid or SPCA1 wild-type plasmid were analyzed by western blot with SPCA1-, cofilin1-, and ADF-specific antibodies.

(D) The medium of these cells was used to detect HRP by chemiluminescence. Error bars indicate mean ± SD of HRP activity in the medium normalized by HRP activity in cell lysates of triplicate measurements from representative experiments. Compared datasets were termed as statistically significant when p values were < 0.01 (**).

(E) In addition, both cell lysates and media were western blotted with anti-Cab45 antibody.

See also Figure S3.

described previously (von Blume et al., 2009). Subsequently, cells were transfected with the $Ca^{2+}$ specific sensor Go-D1cpv, as described above, to measure the $Ca^{2+}$ concentration in the lumen of the TGN. Our results reveal that knockdown of ADF/cofilin1 significantly reduced the $Ca^{2+}$ uptake into the TGN (Figure 4A, red curve). Similar reduction in the Golgi-dependent $Ca^{2+}$ pool was observed with the additional assay using the Fura-2 $Ca^{2+}$ dye (Figure S3A). Importantly, the differences in the $Ca^{2+}$ uptake into the TGN are not due to changes in the $Ca^{2+}$ permeability of the plasma membrane, because both the control and the ADF/cofilin siRNA–treated cells showed a similar response to the withdrawal and subsequent addition of $Ca^{2+}$ to the extracellular bathing solution (Figure S3B). The specificity of the effect of ADF/cofilin knockdown was confirmed by expressing an siRNA-resistant form of cofilin1 (Figure 4A, yellow curve). Taken together, these results suggest a functional interaction between ADF/cofilin and SPCA1. We then tested whether the expression of wild-type SPCA1 in ADF/cofilin1-depleted cells affected the $Ca^{2+}$ pool and cargo sorting at the TGN. The $Ca^{2+}$ level of the TGN and the sorting of HRP and Cab45 were assessed in ADF/cofilin1 knockdown cells transfected with SPCA1-wt and Go-D1cpv. Under these conditions, the $Ca^{2+}$ level of the TGN was restored, and the defects in sorting of HRP and Cab45 induced by ADF/cofilin1 knockdown were rescued (Figures 4B–4E; Figure S3C).

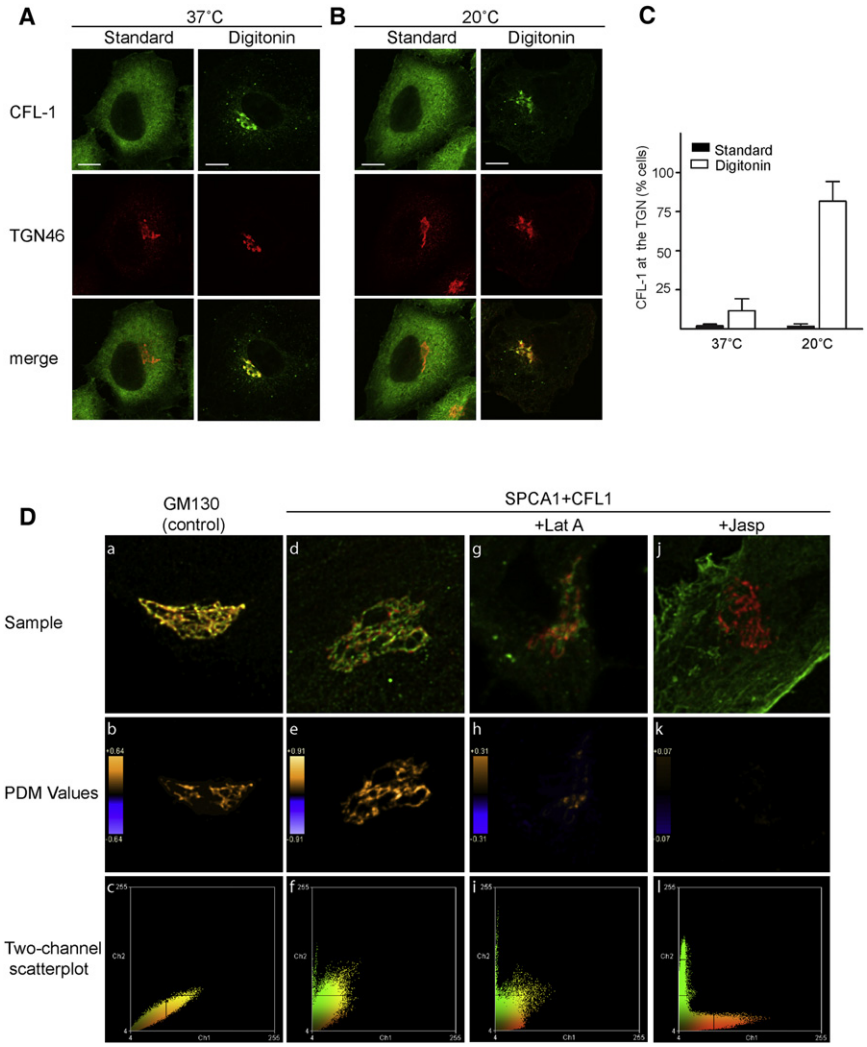


**Figure 5. Cofilin1 Localizes to the TGN**

(A) HeLa cells grown at 37°C were fixed with formaldehyde and permeabilized with Triton X-100 (Standard) or first permeabilized with digitonin, washed, and then fixed with formaldehyde (Digitonin), prior to incubation with cofilin1- and TGN46-specific antibodies.

(B) HeLa cells were cultured at 20°C for 2 hr and then fixed and permeabilized by the standard or digitonin procedure prior to incubation with anti-cofilin1 and TGN46 antibodies.

(C) One hundred cells were randomly counted to determine the colocalization of cofilin1 with TGN46 in cells grown at 37°C or 20°C. Bar graphs represent mean ± SD from at least three independent experiments.

(D) Colocalization analysis of control sample with GM130 staining in both image channels (Alexa 488 and Alexa 555) (a–c). Colocalization analysis of cofilin1 (green) and SPCA1 (red) staining in untreated cells (d–f), cofilin1 (green) and SPCA1 (red) staining in Lat A–treated cells (g–i), and cofilin1 (green) and SPCA1 (red) staining in Jasp-treated cells (j–l). Maximum projections of deconvolved 3D confocal datasets (a, d, and j), maximum projection of 3D confocal dataset (g). Product of the differences from the mean values of the two image channels (covariance) is shown (b, e, h, and k). Scatterplots of the pixel intensities of the two channels are shown (c, f, i, and l).

See also Figure S4.

## Cofilin1 Is Localized to the TGN by an Actin-Dependent Process

The next obvious question was to test whether cofilin1 localizes to the TGN. An anti-cofilin1 antibody was used to visualize its localization by confocal microscopy in HeLa cells. Standard fixation procedure with formaldehyde followed by permeabilization with detergent (Triton) and incubation with an anti-cofilin1 antibody revealed that cofilin1 was distributed throughout the cells (Figure 5A, left panel). We then tested the localization of cofilin1 in cells that were first permeabilized with digitonin, washed extensively to remove the cytosolic proteins, fixed, and then stained with the anti-cofilin1 antibody. This procedure revealed that a pool of cofilin1 colocalized with TGN46, albeit in 10% of the cells (Figure 5A, right panel). We reasoned that the recruitment of cofilin1 to the TGN might be dependent on the secretory activity of the cells. We therefore tested this hypothesis by two independent experimental approaches. First, we investigated whether conditions that accumulate cargo at the TGN by blocking cargo export, such as incubation of cells at 20°C, had any effect on the localization of cofilin1. Interestingly, after a 2-hr block at 20°C and permeabilization with digitonin, more than 80% of the cells showed a TGN-localized cofilin1 (Figures 5B and 5C). Second, HeLa cells stably expressing ss-HRP were tested for cofilin1 localization to the TGN at 37°C. Interestingly, cofilin1 was localized to the TGN in greater than 80% of the cells at 37°C in these cells secreting large amounts of HRP (Figure S4A). This finding raises the possibility that the localization of cofilin1 could potentially be regulated by the secretory capacity of the cells.

As reported previously (von Blume et al., 2009), the ADF/cofilin-dependent sorting of secretory cargo requires dynamic actin. Therefore, the involvement of actin in the localization of cofilin1 at the TGN was tested. To do this, cofilin1 and TGN46 were visualized in untreated (DMSO), Latrunculin A (Lat A, to depolymerize actin filaments) or Jasplakinolide (Jasp, to stabilize actin filaments) treated cells. Remarkably, cofilin1 redistributed from the TGN in cells treated with Lat A or Jasp (Figure S4B).

Phosphorylation of cofilin1 at Ser3 by LIM kinases inhibits the actin-severing activity of cofilin by preventing its binding to actin (Arber et al., 1998). We tested whether the Ser3 phosphorylated (inactive) cofilin1 was localized to the TGN. We examined ss-HRP-expressing HeLa cells at 37°C, the condition under which greater than 80% of cells exhibit cofilin1 localization to the TGN (Figure S4A). The digitonin-permeabilized and washed cells were incubated with a phospho-S3 cofilin1–specific antibody and visualized by fluorescence microscopy. The inactive cofilin was not detected at the TGN (Figure 6A). These data indicate

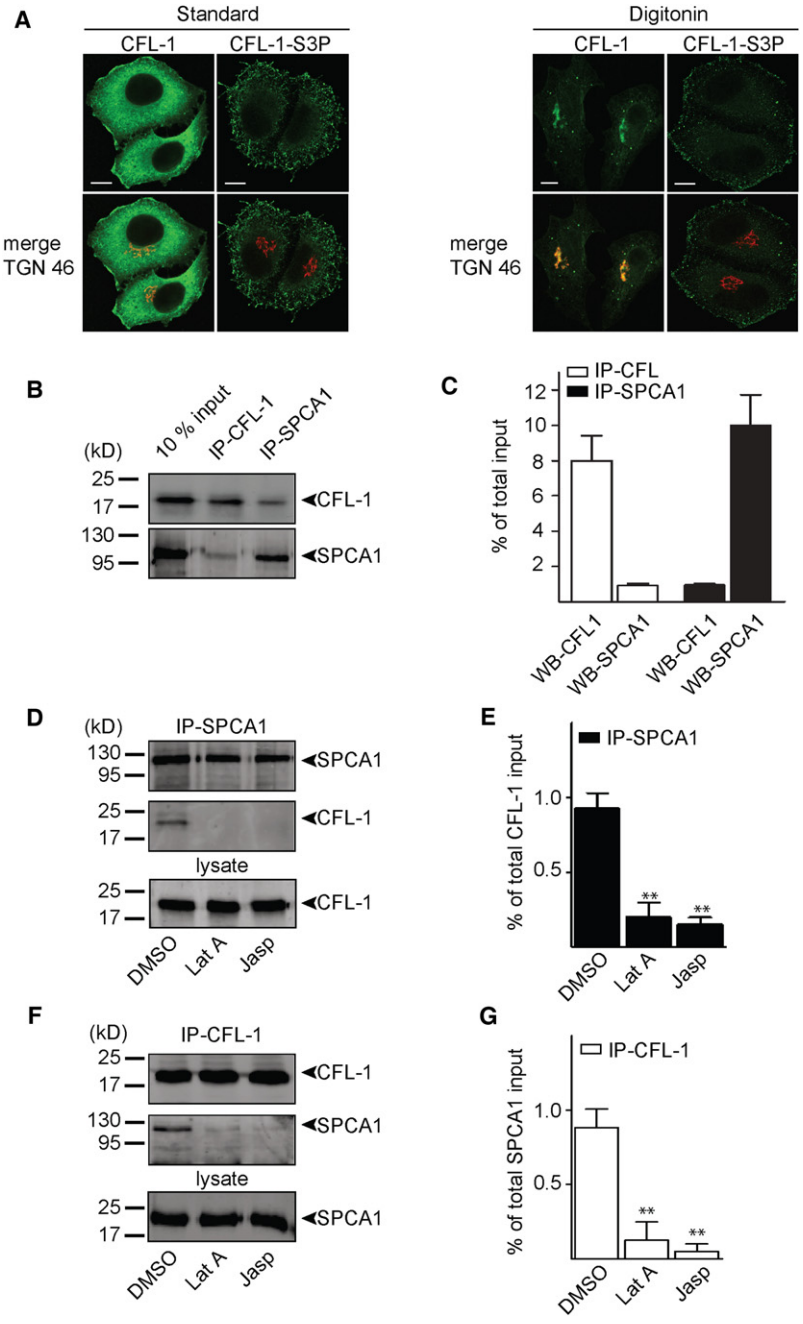


**Figure 6. Cofilin and SPCA1 Bind at the TGN**

(A) HeLa cells stably expressing ss-HRP were grown at 37°C and fixed with formaldehyde and permeabilized with Triton X-100 (Standard) or first were permeabilized with digitonin, washed, and then fixed with formaldehyde (Digitonin), prior to incubation with anti-cofilin1 or anti-cofilin-P-S3 (green) and anti-TGN46 (red) antibodies.

(B) Cofilin1 and SPCA1 were immunoprecipitated from cells. Ten percent total input and the cofilin1 and SPCA1 immunoprecipitates were separated by SDS PAGE and detected by western blotting with SPCA1- and cofilin1-specific antibodies.

(C) IPs shown in (B) were quantified by densitometry using the ImageJ software and were normalized to the total inputs of the proteins. Bar graphs represent the mean ± SD of triplicate experiments. Compared datasets were statistically significant (**) when $p < 0.01$.

(D) HeLa cells were treated with DMSO, Jasp (500 nM), or Lat A (500 nM) for 2 hr. SPCA1 was immunoprecipitated, and IPs were analyzed by SDS page and western blotting with anti-SPCA1 and cofilin1 antibodies.

(F) Cofilin1 was precipitated from the same lysates used in (B), and IPs were analyzed by SDS PAGE and western blotting with anti-SPCA1 and cofilin1 antibodies. (E and G) IPs were quantified by densitometry using the ImageJ software and as described in (B). For SPCA1-IP (E) and for cofilin1-IP (G), bar graphs represent the mean ± SD of triplicate experiments. Compared datasets were statistically significant (**) when $p < 0.01$.

See also Figure S5.

that the pool of cofilin1 localized at the TGN is in the activated form and, therefore, most likely bound to actin. Furthermore, they demonstrate that the localization of the endogenous cofilin1 at the TGN is not created artificially by digitonin-mediated permeabilization of the cells. HeLa cells expressing an HA-tagged version of cofilin1 were stained with an anti-HA as well as an anti-SPCA1 specific antibody. Cofilin1 showed a colocalization with SPCA1. Permeabilization with digitonin and washing did not change the location or the organization of the SPCA1 at the TGN (Figure S4C). In the next step, the colocalization between cofilin1 and SPCA1 at the TGN was quantified under the different conditions using 3D confocal microscopy and subsequent software analysis. To test the accuracy of the measurement approach, control samples of HeLa cells were stained with a primary antibody against the Golgi-associated protein GM130 and then incubated with a mixture of secondary antibodies conjugated to Alexa 488 and Alexa 555. This should reveal complete colocalization, and the measured values were accordingly close to the theoretical maximum (Figures 5Da–5Dc; Figure S4D). Then, cofilin1 and SPCA1 were visualized with specific antibodies in untreated cells and cells treated with either Lat A or Jasp. In control conditions, the staining of cofilin1 and SPCA1 revealed substantial but not complete overlap (Figures 5Dd–5Df), as evidenced by the value of the Pearson correlation coefficient (Figure S4D), and substantial dependence, as evidenced by the value of the intensity correlation quotient (Figure S4D). Upon treatment with Lat A, the overlap of the staining was reduced as cofilin1 was redistributed away from the TGN, whereas the localization of the transmembrane protein SPCA1 remained unaffected (Figure 5Dg). The partial dependence of the staining was, however, not completely abolished, because a small pool of cofilin1 with moderate overlap with SPCA1 was still observed under such conditions (Figures 5Dh and 5Di; Figure S4D). Treatment with Jasp caused almost complete loss of the cofilin1 from the TGN without affecting the location of SPCA1 (Figure 5Dj). Accordingly, both the colocalization and the dependence value of the

staining became random (~0) (Figures 5Dj–5Dl; Figure S4D). These findings confirm the involvement of dynamic actin in the localization of cofilin1 at the TGN.

### Dynamic Actin Is Required for Cofilin1-SPCA1 Interaction at the TGN

As shown above, SPCA1 and cofilin1 colocalize at the TGN. In the next step, their physical interaction was assessed by coimmunoprecipitation procedures. Cofilin1 and SPCA1 were immunoprecipitated with specific antibodies. SPCA1 was detected in the cofilin1 precipitate. Cofilin1 was also detected by western blot in SPCA1 immunoprecipitated from the HeLa cell lysates (Figure 6B). As shown in Figure 6C, 8% of total cofilin1 was immunoprecipitated from the cells and 0.8% of total SPCA1 was detectable in the complex. Similar results were obtained when SPCA1 was immunoprecipitated and cofilin1 was detected. The antibody precipitated 10% of total SPCA1, which comimmunoprecipitated with 1% of total cofilin1.

As described above, treatment with actin filament–perturbing agents, Lat A and Jasp, dissociated cofilin1 from the TGN. Thus, dynamic actin is required for the association and therefore interaction with SPCA1. Lysates of HeLa cells treated with Lat A or Jasp were immunoprecipitated with anti-cofilin1 or SPCA1 antibodies, and the immunoprecipitates were western blotted with anti-cofilin1 and SPCA1 antibodies, respectively. Clearly, treatment with Lat A or Jasp dramatically reduced the coprecipitation of cofilin1 with SPCA1 (Figures 6D–6G).

The interaction between SPCA1 and cofilin1 was also tested by FRET. In samples colabeled for SPCA1 and cofilin1 with secondary antibodies, a low FRET interaction could consistently be detected by acceptor photobleaching (Figure S5). This finding suggests that these two proteins are localized within the nanometer range at the TGN.

### SPCA1 Localization to the TGN Is Necessary for the ADF/Cofilin-Mediated $Ca^{2+}$ Homeostasis and Protein Sorting

Thus far, our findings revealed that cofilin1 is localized to the TGN and forms a complex with SPCA1 through dynamic actin. To further strengthen this proposal, we asked whether a form of SPCA1 arrested in the ER was capable of interacting with cofilin1 and had any role in $Ca^{2+}$ import and cargo sorting at the TGN. SPCA1 contains a C-terminal valine, which has been reported to be an essential motif for the export of some proteins from the ER (Wendeler et al., 2007). The C-terminal valine 919 of SPCA1 was replaced with alanine. HA-tagged SPCA1-wt and HA-SPCA1-V919A were expressed in HeLa cells and visualized by confocal microscopy with an anti-HA antibody. HA-SPCA1 wild-type was clearly localized at the TGN, whereas the valine mutant was retained in the ER (Figure 7A). This result corroborates the role of the C-terminal valine (V919) of SPCA1 as an ER export motif. HeLa cells depleted of endogenous SPCA1 by siRNA (as described above) were then transfected with siRNA resistant SPCA1-wt and -V919A. The TGN-targeted $Ca^{2+}$ sensor Go-D1cpv, as described above, was used to measure the $Ca^{2+}$ levels in the TGN. As shown in Figure 7C, SPCA1-wt rescued the $Ca^{2+}$ level of cells depleted of endogenous SPCA1, but not SPCA1-V919A. An identical result was obtained when cytosolic [$Ca^{2+}$] was measured with Fura-2 (Figure S6). The same experiments were performed in cells transfected with ADF and cofilin1 siRNAs. Calcium import into the TGN of ADF/cofilin1 knockdown cells was rescued by overexpression of SPCA1 wild-type (Figure 4B) but not by SPCA1-V919A (Figure 7D).

We then monitored the effect on HRP secretion in cells treated with siRNA-resistant SPCA1-wt and -V919A in SPCA1- or ADF/cofilin1-depleted cells. The sorting defect induced by the knockdown of SPCA1 or ADF/cofilin1 was rescued by SPCA1-wt but not by the ER-retained mutant SPCA1-V919A (Figures 7E and 7F).

Finally, cells transfected with control or SPCA1 siRNA were cotransfected with control, SPCA1-wt, or SPCA1-V919A plasmids. Cofilin1 was immunoprecipitated, and the immunoprecipitates and cell lysates were assessed with an anti-SPCA1 antibody. As shown in Figure 7B, cofilin1 coimmunoprecipitated with the endogenous SPCA1 and SPCA1-wt but not with the ER-retained mutant of SPCA1. These findings strongly indicate that SPCA1 localization at the TGN is required for $Ca^{2+}$ homeostasis, interaction with cofilin1, and secretory cargo sorting.

## DISCUSSION

A genomewide screen to identify new components of the secretory pathway led to the identification of the actin-severing protein twinstar or ADF/cofilin (Bard et al., 2006). Subsequent studies revealed that ADF/cofilin was in fact required for sorting secretory cargo at the TGN. Knockdown of ADF and cofilin1 (two orthologs of *Drosophila* twinstar expressed in HeLa cells) inhibited export of ss-HRP from the TGN. Surprisingly, secretion of a number of other secretory proteins was unaffected, and the lysosomal hydrolase Cathepsin D and the $Ca^{2+}$-binding soluble Golgi resident protein Cab45 were secreted from cells. The defects in sorting could be partially rescued by treatment of cells with the actin depolymerizing agent Lat A. However, it is important to note that Lat A treatment alone caused a sorting defect, implying the involvement of dynamic actin in the sorting of secretory cargo. On the basis of these findings, we proposed that ADF/cofilin and dynamic actin were required for sorting of secretory cargo at the TGN (von Blume et al., 2009). How would the cytoplasmic ADF/cofilin communicate with the lumenal secretory cargo across the membrane of the TGN?

### Cofilin1 Regulates SPCA1-Dependent $Ca^{2+}$ Uptake into the TGN

Our data indicate that $Ca^{2+}$ import into the TGN is mediated by the interaction of ADF/cofilin with the transmembrane $Ca^{2+}$ ATPase SPCA1. Knockdown of ADF and cofilin1 in HeLa cells inhibited $Ca^{2+}$ import into the TGN and caused missorting, which was rescued by expressing an siRNA-resistant cofilin1 or overexpressing SPCA1 in the TGN. SPCA1 is therefore the previously hypothesized molecular sorter that connects the lumenal secretory cargo to the cytoplasmically localized ADF/cofilin at the TGN (von Blume et al., 2009). The role of SPCA1 in import of $Ca^{2+}$ into the TGN is well documented (Lissandron et al., 2010; Missiaen et al., 2007); our findings reveal the significance of this reaction in the sorting of secretory cargo.

### Role of Dynamic Actin-ADF/Cofilin-SPCA1-$Ca^{2+}$ in Cargo Sorting at the TGN

The localization of cofilin1 at the TGN requires dynamic actin. Dynamic actin therefore fits the properties expected of a linker

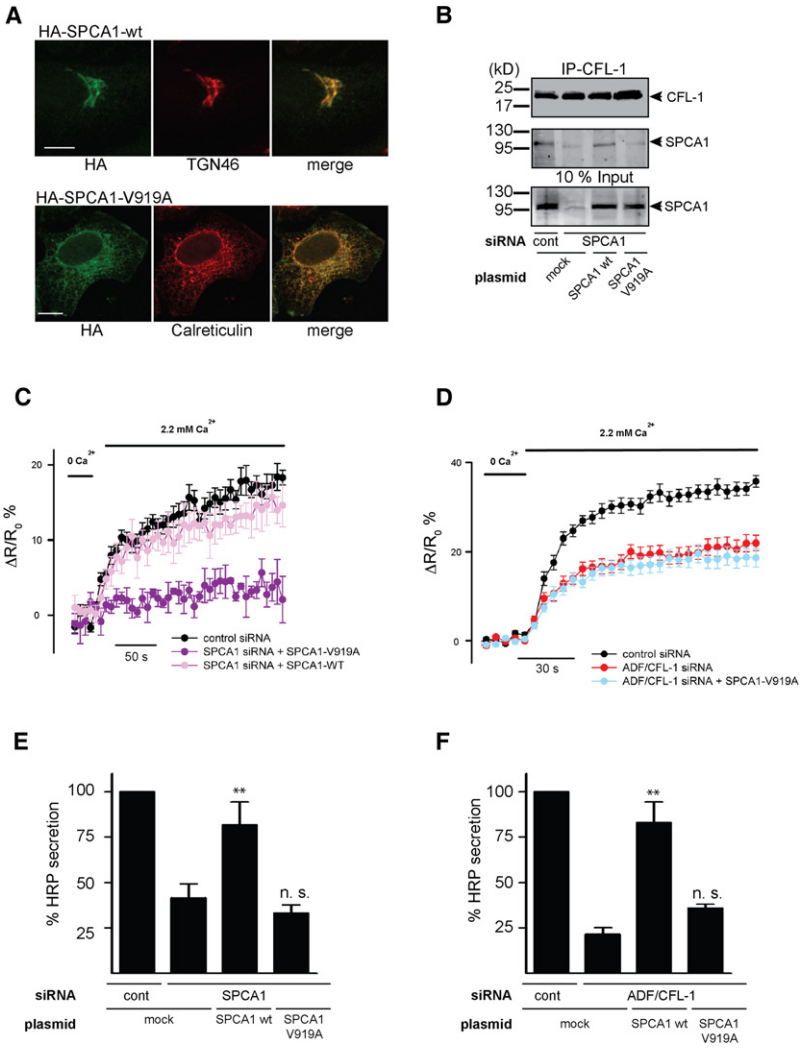


**Figure 7. SPCA1 Localization to the TGN Is Necessary for the ADF/Cofilin-Mediated $Ca^{2+}$ Homeostasis and Protein Sorting**

(A) HeLa cells were transfected with HA-SPCA1 wild-type and HA-SPCA1-V919A. Proteins were visualized by staining with an anti-HA antibody and anti-TGN46 (for HA-SPCA1 wild-type) or anti-Calreticulin (for HA-SPCA1-V919A) antibodies, and images were taken by confocal microscopy. Size bars indicate 5 μm.

(B) Cells were incubated with control or SPCA1 siRNAs and subsequently transfected with a mock plasmid, SPCA1 wild-type, or SPCA1 V919A. Cofilin1 was immunoprecipitated from cells, and IPs were analyzed by SDS page and western blotting with SPCA1- and cofilin1-specific antibodies.

(C) HeLa cells treated with control or SPCA1-specific siRNAs were transfected with a control plasmid (n = 36), SPCA1 siRNA–resistant wild-type (n = 11), or SPCA1 siRNA–resistant V919A (n = 3), and the TGN-specific $Ca^{2+}$ FRET sensor GoD1cpv. TGN measurements were performed as described in previous figures. Mean maximum values after readdition of $Ca^{2+}$ were statistically different between control and SPCA1 siRNA–resistant V919A siRNA (19 ± 1% and 2 ± 0.7%, respectively; $p < 0.01$) but not between control and SPCA1 siRNA–resistant wild-type (14 ± 1%; $p > 0.05$).

(D) $Ca^{2+}$ entry into the TGN was measured using the Go-D1cpv probe in cells treated with control (n = 12) or ADF and cofilin1 siRNAs and transfected with a mock plasmid (n = 7) or SPCA1 V919A plasmid (n = 7). Mean maximum values after readdition of $Ca^{2+}$ were statistically different between control (35 ± 1%) and both ADF/ cofilin1 siRNA (21 ± 1%) or ADF/cofilin siRNA + SPCA1 V919A plasmid (19 ± 1%; $p > 0.05$).

(E) Cells were treated as described in (C) and the medium was used to detect HRP by chemiluminescence.

(F) Cells were treated as described in (D) and the medium was used to detect HRP by chemiluminescence. Error bars indicate mean ± SD of HRP activity in the medium normalized by HRP activity in cell lysates of triplicate measurements from representative experiments. Compared datasets were termed as statistically significant when $p < 0.01$ (**).

See also Figure S6.

to connect ADF/cofilin on the cytoplasmic side of the TGN with secretory cargo in the lumen via the transmembrane $Ca^{2+}$ ATPase SPCA1. How does this arrangement of actin-ADF/cofilin-SPCA1 help sort cargo in the TGN? We have shown previously that activated ADF/cofilin, which severs actin, is necessary for sorting secretory cargo (von Blume et al., 2009). The activity of ADF/cofilin is regulated by LIM kinase (LIMK)–mediated phosphorylation (inactivates ADF/cofilin) and dephosporylation by slingshot (SSH, activates ADF/cofilin) (Rosso et al., 2004). LIMK has been localized to the TGN and shown to be involved in the formation of TGN to cell surface transport carriers that contain cargo destined to the apical surface in polarized cells (Salvarezza et al., 2009). Our data indicate that perturbing the activity of ADF/cofilin through its regulators LIMK and SSH affects cargo sorting without affecting the process of transport carrier biogenesis per se, as shown previously (von Blume et al., 2009). We suggest that actin exists in a dynamic state at the TGN. The actin filaments bind SPCA1 and, in this form, SPCA1 is functionally inactive. The active form of ADF/cofilin binds to the TGN and severs actin filaments. This exposes and activates SPCA1, which can then pump $Ca^{2+}$ into the lumen of the TGN (see Graphical Abstract). At present, we cannot conclude whether this is the result of SPCA1 activation by hitherto unknown cytoplasmic machinery or because of the release from a possible inhibitory effect of actin filaments. Regardless, this would explain our findings on the effect of actin-depolymerizing agent Lat A, which partially rescues the sorting defects created by ADF/cofilin1 knockdown. This would also explain the fact that overexpression of TGN-localized wild-type SPCA1 ameliorated the sorting defect created by ADF/cofilin1 knockdown. In this case, the overexpressed SPCA1 is most likely not fully captured into the actin network and therefore is capable of pumping $Ca^{2+}$ into the TGN. In this context, it is important to note the data on the connections between ion transporters and dynamic actin (Chun and Santella, 2009; Hryciw et al., 2003; Lee et al., 2001) and the recent data pointing to a role of SPCA2 (an isoform of SPCA1) in the regulation of plasma membrane ion channels (Feng et al., 2010).

In sum, our results demonstrate the role of actin-ADF/cofilin-SPCA1–dependent $Ca^{2+}$ pumping into the TGN in cargo sorting. The advantage of an actin-ADF/cofilin-SPCA1-$Ca^{2+}$–dependent

sorting process, we suggest, is its independence from a specific receptor-mediated sorting, such as the M6PR-mediated sorting of soluble lysosomal hydrolases. This might also explain why a specific cargo receptor for secreted proteins has not been identified thus far at the TGN. Other secretory proteins might depend on parameters such as the pH or binding to specific lipids for their sorting and export from the TGN. It is also worth noting that mutations in *PMR1*, the SPCA1 ortholog in *Saccharomyces cerevisiae*, affected sorting of the vacuolar protein CPY and pheromone maturation. These defects were corrected by growing yeast in high $Ca^{2+}$ (Antebi and Fink, 1992). The $Ca^{2+}$ dependent sorting of secretory cargo at the TGN might therefore be more highly conserved than currently appreciated.

## EXPERIMENTAL PROCEDURES

### Antibodies, Plasmids, and Cell Culture

We kindly thank Dr. Wuytack (KU Leuven, Belgium) for the generous gift of the SPCA1 wild-type plasmid and the anti-SPCA1 polyclonal antibody, and Dr. Tulio Pozzan for the generous gift of the $Ca^{2+}$ sensor Go-D1cpv. Monoclonal antibody against ATP2C1 (SPCA1) was from AbD Serotec; we also used monoclonal antibodies against cofilin1 and HRP, polyclonal antibodies against cofilin1 and cofilin-P-S3 (Abcam), polyclonal anti-ADF and monoclonal anti-β-actin (Sigma Aaldrich), sheep anti–human TGN46 (AbD Serotec), monoclonal anti–Cathepsin D antibody (Cell signaling), anti-Cab45 monoclonal antibody (Transduction Laboratories), and anti-HA antibody (Covance). Protein A Sepharose was from GE Healthcare. Secondary antibodies for immunofluorescence microscopy and western blotting were from Life Technologies. Lat A was from Calbiochem and Jasp was from Life Technologies.

### Cell Culture and Transfection

HeLa cells and HeLa cells stably expressing ss-HRP (see details in Supplemental Experimental Procedures) were grown in DMEM (PAA) containing 10% FCS at 37°C with 7% $CO_2$. Cells were transfected with Lipofectamine2000 (Life Technologies), FuGENE 6 (Roche), Nucleofector (Cell Line KitV solution, Amaxa), or TransIT-HeLaMONSTER (Mirus) following the manufacturers' recommendation.

### ss-HRP Transport Assay

HeLa cells stably expressing ss-HRP were transfected with siRNA (see details in Supplemental Experimental Procedures) and processed for HRP secretion as described previously (Bard et al., 2006). Fifty microliters of the medium was harvested 48 hr after the initial siRNA transfection, and the HRP activity was measured as described previously (Bossard et al., 2007). For normalization, cells were lysed with 0.5% Triton X-100, and internal HRP activity was measured. For rescue experiments, siRNA-treated cells were transfected with a pcDNA3 (control plasmid) or pcDNA3-SPCA1 12 hr after the initial siRNA transfection.

### Visualizing Intracellular HRP

Thirty hours after transfection with siRNA, HeLa cells stably expressing ss-HRP were incubated with 100 μg/ml cycloheximide for 2 hr at 20°C. After shifting to 32°C, cells were fixed at different time points indicated in the figures, incubated with primary antibodies (anti HRP), and processed for immunofluorescence microscopy.

### Cab45 and Cathepsin D Sorting Assays

Control or siRNA-transfected cells were washed five times with serum-free medium. The cells were then grown in serum-free medium and after 2 hr, the medium was collected. Cells were counted and lysed as described previously (von Blume et al., 2009). Media from control and siRNA treated cells were filtered using a 0.45-μm filter (Millipore), centrifuged at 5000× g for 15 min, and the resulting supernatant was then centrifuged at 100,000× g for 2 hr. Samples were concentrated using a 3000-Da molecular mass cutoff spin column (Millipore) and subsequently separated by SDS-PAGE and western blotted with Cathepsin D and Cab45 antibodies, respectively.

### Cofilin Localization Assay

HeLa ATTC cells and HeLa cells stably expressing ss-HRP were grown on 12-mm glass coverslips and were either processed directly or incubated at 20°C for 2 hr. Cells were then fixed in 4% formaldehyde, permeabilized, and blocked for 1 hr in standard buffer (0.2% Triton X-100, 0.5% SDS, and 4% BSA) before processing for confocal microscopy with a cofilin1 or HA antibody (for HA-cofilin1-overexpressing cells). Alternatively, the coverslips were washed twice with ice-cold KHM buffer (125 mM potassium acetate, 25 mM HEPES [pH 7.2], and 2.5 mM magnesium acetate). Cells were then permeabilized by incubating the coverslips on ice in 0.5 ml of KHM containing 30 μg/ml digitonin for 5 min and then washed for 7 min at room temperature with KHM buffer. Cells were subsequently fixed and processed for immunofluorescence microscopy.

### Immunofluorescence Microscopy

All fixed samples were analyzed with a Leica SPE confocal microscope using the 63× Plan Apo NA1.3 objective. For the detection of Alexa 555 and Alexa 594, the 532 nm and for Alexa 488, the 488 nm laserline was applied. Pictures were acquired using the Leica software and converted to TIFF files in Image J (version 1.37).

### Colocalization Analysis by 3D Microscopy

The proteins chosen for the localization comparison were incubated with specific antibodies for the respective proteins followed by secondary antibodies labeled with Alexa 488 and Alexa 555. High-resolution 3D stacks were then acquired of multiple cells in each sample on a Leica SP5 II confocal microscope with a 100× 1.4 NA Plan Apo objective. For all further processing steps, the processing program ImageJ (version 1.43r) and its plugins were used. Datasets were background corrected by subtraction of the intensities measured in empty areas of the image, noise-filtered using a Gaussian filter, and thresholded to exclude background areas before colocalization analysis. The chromatic aberration for the objective was determined and a detected subresolution z-shift (125 nm) corrected by translating the affected channel slightly in z. To determine the Pearson coefficient and the intensity correlation quotient, the plugin "Intensity Correlation Analysis" was used. For visualization of the scattergrams, images were taken from the plugin "Manders Coefficients." To test the accuracy of the measurement approach, control samples were stained with a primary antibody against the Golgi protein GM130 that was then visualized with a mixture of secondary antibodies conjugated to Alexa 488 and Alexa 555. This should provide full colocalization, and the measured values were accordingly close to the theoretical maximum. Sets of untreated and treated cells were then analyzed identically (minimum, 10 3D stacks for each condition) for their cofilin1 (Alexa 488) and SPCA1 (Alexa 555) distributions.

### Immunoprecipitations

Untransfected HeLa cells stably expressing ss-HRP or HeLa cells stably expressing ss-HRP that were transfected with control or SPCA1-specific siRNA were lysed in 50 mM Tris (pH 7.4), 150 mM NaCl, 0.5% Triton X-100, and protease inhibitors for 30 min at 4°C. After centrifugation at 13,000 rpm for 10 min, lysates were again cleared by 100,000 g for 30 min. Subsequently, lysates were incubated with the primary antibody (1:100) for 30 min at 20°C. After 2 hr incubation at 4°C, protein A Sepharose was added, and the samples were incubated over night. Immobilized proteins were released by boiling the sample in Laemmli buffer and were analyzed by SDS-PAGE.

### Mass Spectrometry

Immunoprecipitated proteins were separated by 1D-gel electrophoresis and the bands were excised and trypsinized (Promega) following established protocols (Shevchenko et al., 2006). Extracted peptides were analyzed by reversed phase HPLC (Agilent 1200 nano flow pump, Agilent Technologies) coupled to a mass spectrometer (Orbitrap XL, ThermoFisher). MS/MS data were extracted using ProeomeDiscoverer 1.2.208 (ThermoFisher) and queried against IPI Human using Mascot version 2.2 (Matrix Science Inc.). Proteins were filtered using $p > 0.05$.

### $Ca^{2+}$ Imaging

$Ca^{2+}$ entry into the TGN was measured as described by Lissandron et al. (2010). Measurements of [$Ca^{2+}$] in the TGN were carried out using a fluorescent $Ca^{2+}$ indicator (Go-D1cpv) based on the efficiency of FRET between CFP and YFP

fluorescent proteins linked by a modified calmodulin and calmodulin-binding domain. This genetically encoded $Ca^{2+}$ indicator was targeted to the TGN (Lissandron et al., 2010). $Ca^{2+}$ entry into the TGN was measured in $Ca^{2+}$-depleted cells following 1 hr incubation at 4°C in a $Ca^{2+}$-free solution (140 mM NaCl, 5 mM KCl, 1.2 mM $MgCl_2$, 5 mM glucose, 10 mM HEPES, and 0.5 mM EGTA [300 mosmol/l, pH 7.4, with Tris] with 1 μM ionomycin; Lissandron et al., 2010). Then cells were washed twice with 2% BSA $Ca^{2+}$-free solution. Images were generated following excitation at 428 nm and emission captured at 520 nm (YFP) and 480 nm (CFP) using a Leica TCS SP5 inverted confocal microscope (63× oil objective). Images were captured at 0.7 Hz at room temperature. Fluorescent signals reflecting TGN [$Ca^{2+}$] were presented as $\Delta R/R_0$, where $R_0$ is the value obtained before addition of 2.2 mM $Ca^{2+}$ to the cells bathing solution. When required, siRNAs were transfected using Hiperfect, and 48 hr later the Go-D1cpv $Ca^{2+}$ probe with or without different SPCA1 constructs were transfected using TransIT-HeLaMONSTER reagent. Cytosolic $Ca^{2+}$ measurements using Fura-2 were also performed as described elsewhere (Cantero-Recasens et al., 2010) (Supplemental Experimental Procedures).

### Statistical Analysis

Statistical significance was tested in an unpaired Student's t test or ANOVA using the Graph Pad Prism, SigmaPlot, and Origin software. Bonferroni's test was used for post hoc comparison of means. Compared datasets were termed as statistically significant when $p < 0.01$ (**).

## SUPPLEMENTAL INFORMATION

Supplemental Information includes six figures and Supplemental Experimental Procedures and can be found with this article online at doi:10.1016/j.devcel.2011.03.014.

## ACKNOWLEDGMENTS

Members of the Malhotra lab are thanked for valuable discussion. Julia von Blume is funded by a long-term EMBO postdoctoral fellowship. Vivek Malhotra is an Institucio Catalana de Recerca I Estudis Avancats (ICREA) professor at the Center for Genomic Regulation and the work in his lab is funded by grants from Plan Nacional (BFU2008-00414), Consolider (CSD2009-00016), and AGAUR SGR2009-1488 Grups de Recerca Emergents (AGAUR-Catalan government). Miguel A. Valverde is the recipient of an ICREA Academia Award and the work in his lab was supported by Spanish Ministry of Science and Innovation, FEDER Funds and Plan E (SAF2009-09848, Red HERACLES RD06/0009); Generalitat de Catalunya (2009SGR-1369); and Fundació la Marató de TV3 (080430). We thank Dr. Frank Wuytack for SPCA1 reagents and Dr. Tulio Pozzan for the $Ca^{2+}$ sensor. We thank Stefan Terjung from EMBL (Heidelberg, Germany) for the help with deconvolution and image processing and Dr. Rajini Rao for valuable discussions. The MS-based protein identification proteomic analysis was carried out in the Joint UPF/CRG Proteomics Facility at Parc de Recerca Biomèdica de Barcelona, a member of the ProteoRed network.

Received: July 23, 2010
Revised: February 22, 2011
Accepted: March 15, 2011
Published: May 16, 2011

## REFERENCES

Antebi, A., and Fink, G.R. (1992). The yeast Ca(2+)-ATPase homologue, PMR1, is required for normal Golgi function and localizes in a novel Golgi-like distribution. Mol. Biol. Cell *3*, 633–654.

Arber, S., Barbayannis, F.A., Hanser, H., Schneider, C., Stanyon, C.A., Bernard, O., and Caroni, P. (1998). Regulation of actin dynamics through phosphorylation of cofilin by LIM-kinase. Nature *393*, 805–809.

Baranski, T.J., Faust, P.L., and Kornfeld, S. (1990). Generation of a lysosomal enzyme targeting signal in the secretory protein pepsinogen. Cell *63*, 281–291.

Bard, F., Casano, L., Mallabiabarrena, A., Wallace, E., Saito, K., Kitayama, H., Guizzunti, G., Hu, Y., Wendler, F., Dasgupta, R., et al. (2006). Functional genomics reveals genes involved in protein secretion and Golgi organization. Nature *439*, 604–607.

Bossard, C., Bresson, D., Polishchuk, R.S., and Malhotra, V. (2007). Dimeric PKD regulates membrane fission to form transport carriers at the TGN. J. Cell Biol. *179*, 1123–1131.

Cantero-Recasens, G., Fandos, C., Rubio-Moscardo, F., Valverde, M.A., and Vicente, R. (2010). The asthma-associated ORMDL3 gene product regulates endoplasmic reticulum-mediated calcium signaling and cellular stress. Hum. Mol. Genet. *19*, 111–121.

Chun, J.T., and Santella, L. (2009). Roles of the actin-binding proteins in intracellular Ca2+ signalling. Acta Physiol. (Oxf.) *195*, 61–70.

Feng, M., Grice, D.M., Faddy, H.M., Nguyen, N., Leitch, S., Wang, Y., Muend, S., Kenny, P.A., Sukumar, S., Roberts-Thomson, S.J., et al. (2010). Store-independent activation of Orai1 by SPCA2 in mammary tumors. Cell *143*, 84–98.

Gunteski-Hamblin, A.M., Clarke, D.M., and Shull, G.E. (1992). Molecular cloning and tissue distribution of alternatively spliced mRNAs encoding possible mammalian homologues of the yeast secretory pathway calcium pump. Biochemistry *31*, 7600–7608.

Hryciw, D.H., Wang, Y., Devuyst, O., Pollock, C.A., Poronnik, P., and Guggino, W.B. (2003). Cofilin interacts with ClC-5 and regulates albumin uptake in proximal tubule cell lines. J. Biol. Chem. *278*, 40169–40176.

Lee, K., Jung, J., Kim, M., and Guidotti, G. (2001). Interaction of the alpha subunit of Na,K-ATPase with cofilin. Biochem. J. *353*, 377–385.

Lewis, M.J., and Pelham, H.R. (1990). A human homologue of the yeast HDEL receptor. Nature *348*, 162–163.

Lissandron, V., Podini, P., Pizzo, P., and Pozzan, T. (2010). Unique characteristics of Ca2+ homeostasis of the trans-Golgi compartment. Proc. Natl. Acad. Sci. USA *107*, 9198–9203.

Missiaen, L., Dode, L., Vanoevelen, J., Raeymaekers, L., and Wuytack, F. (2007). Calcium in the Golgi apparatus. Cell Calcium *41*, 405–416.

Pfeffer, S.R. (2007). Unsolved mysteries in membrane traffic. Annu. Rev. Biochem. *76*, 629–645.

Rosso, S., Bollati, F., Bisbal, M., Peretti, D., Sumi, T., Nakamura, T., Quiroga, S., Ferreira, A., and Caceres, A. (2004). LIMK1 regulates Golgi dynamics, traffic of Golgi-derived vesicles, and process extension in primary cultured neurons. Mol. Biol. Cell *15*, 3433–3449.

Salvarezza, S.B., Deborde, S., Schreiner, R., Campagne, F., Kessels, M.M., Qualmann, B., Caceres, A., Kreitzer, G., and Rodriguez-Boulan, E. (2009). LIM kinase 1 and cofilin regulate actin filament population required for dynamin-dependent apical carrier fission from the trans-Golgi network. Mol. Biol. Cell *20*, 438–451.

Sepulveda, M.R., Vanoevelen, J., Raeymaekers, L., Mata, A.M., and Wuytack, F. (2009). Silencing the SPCA1 (secretory pathway Ca2+-ATPase isoform 1) impairs Ca2+ homeostasis in the Golgi and disturbs neural polarity. J. Neurosci. *29*, 12174–12182.

Shevchenko, A., Tomas, H., Havlis, J., Olsen, J.V., and Mann, M. (2006). In-gel digestion for mass spectrometric characterization of proteins and proteomes. Nat. Protoc. *1*, 2856–2860.

Vanoevelen, J., Dode, L., Van Baelen, K., Fairclough, R.J., Missiaen, L., Raeymaekers, L., and Wuytack, F. (2005a). The secretory pathway Ca2+/Mn2+-ATPase 2 is a Golgi-localized pump with high affinity for Ca2+ ions. J. Biol. Chem. *280*, 22800–22808.

Vanoevelen, J., Raeymaekers, L., Dode, L., Parys, J.B., De Smedt, H., Callewaert, G., Wuytack, F., and Missiaen, L. (2005b). Cytosolic Ca2+ signals depending on the functional state of the Golgi in HeLa cells. Cell Calcium *38*, 489–495.

von Blume, J., Duran, J.M., Forlanelli, E., Alleaume, A.M., Egorov, M., Polishchuk, R., Molina, H., and Malhotra, V. (2009). Actin remodeling by ADF/cofilin is required for cargo sorting at the trans-Golgi network. J. Cell Biol. *187*, 1055–1069.

Wendeler, M.W., Paccaud, J.P., and Hauri, H.P. (2007). Role of Sec24 isoforms in selective export of membrane proteins from the endoplasmic reticulum. EMBO Rep. *8*, 258–264.